Dual-Tracer Measurements of Concentration Profiles in the Aqueous Mass Boundary Layer

Thomas Münsterer[1], *Hans Jürgen Mayer*[1], *and Bernd Jähne*[2,3]

[1]Institute for Environmental Physics, University of Heidelberg
Im Neuenheimer Feld 366, 69120 Heidelberg, Germany
email: Thomas.Muensterer@iwr.uni-heidelberg.de
[2]Scripps Institution of Oceanography, Physical Oceanography Res. Div.
La Jolla, CA 92093-0230, USA, email: bjaehne@ucsd.edu
[3]Interdisciplinary Center for Scientific Computing, University of Heidelberg
Im Neuenheimer Feld 368, 69120 Heidelberg, Germany

Abstract

A combination of two laser-induced fluorescence (LIF) techniques for measurements of vertical concentration profiles of dissolved gases and thus the investigation of micro-turbulence in the aqueous mass boundary layer at a free interface is presented. The first one uses an acid-base reaction of the fluorescence indicator fluorescein at the water surface to visualize the concentration profiles. The second one uses fluorescence quenching of pyrenebutyric acid by oxygen. Both experiments are done simultaneously at the same location.

The advantage of a combined experiment is that the two techniques utilized here to visualize the concentration profiles are caused by different independent physical effects, i.e. an acid-base reaction and the fluorescence quenching by oxygen. Simultaneous measurements can help to detect possible systematic errors and offer the chance to learn more about the underlying gas exchange mechanisms.

Experiments performed at the circular facility of the University of Heidelberg using a surfactant to suppress waves are presented. For three wind speeds the mean and fluctuating boundary layer properties are investigated.

1 Introduction

Our understanding of the parameters influencing air-sea gas exchange has increased considerably in recent years, however, little is known about the mechanisms that control this process. There is limited data available with which to evaluate the different gas exchange models. To understand gas exchange mechanisms it is essential to investigate the processes within the aqueous *mass boundary layer*. This paper describes two laser induced fluorescence (LIF) techniques which measure vertical *concentration profiles* with high temporal and spatial resolution. One technique uses the dye *fluorescein*. A less fluorescent species of fluorescein anions is generated at the water surface through a reaction with an acidic gas. These species undergo

B. Jähne and E. Monahan (eds.), Air-Water Gas Transfer, © *1995 by AEON Verlag*

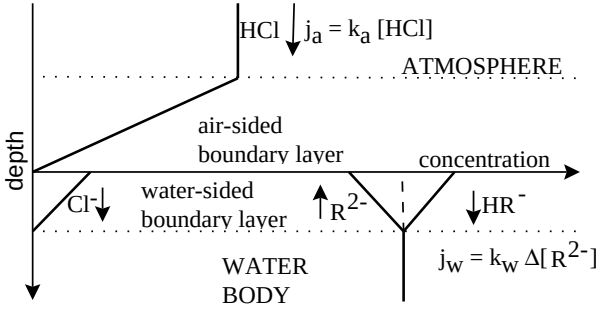

Figure 1: Schematic representation of the vertical concentration profiles at the air-water interface, when HCl is absorbed by a buffer solution.

no further reactions and are transferred into the bulk water flow. The second technique uses the dye pyrene butyric acid, whose *fluorescence* is quenched by *dissolved oxygen*. The research described in this paper was undertaken to make combined measurements with the two techniques at the same time and at the same location. Combined measurements have the advantage of allowing identification of systematic errors (the chemical and physical effects are very different) and investigation of the Schmidt number dependency of the underlying gas exchange mechanisms ($Sc \approx 2500$ for fluorescein and $Sc \approx 470$ for oxygen).

2 LIF Principles

This section describes how the two LIF techniques allow visualization of the concentration profiles in the aqueous mass boundary layer. It is crucial that the fluorescence intensity is a function solely of the concentration of the exchange component. This is fulfilled for both techniques.

2.1 The Fluorescein Method

The fluorescein technique uses an acid-base reaction at the interface to generate fluorescent molecules to visualize the concentration profiles (Figure 1). The *fluorescent indicator* sodium fluorescein is used at its buffer point in a 2×10^{-5} M solution. At the buffer point the solution contains equal concentrations of the two ionic species of fluorescein (abbreviated here as HR^- and R^{2-}). An *acid gas*, e. g. Hcl, is then injected into an air-tight wind/wave facility in ppm concentration levels. The water surface acts as a perfect sink for the HCl. The HCl gas dissociates instantaneously and protonates the fluorescein anions at the water surface generating an excess number of the less fluorescent singly charged fluorescein anion HR^-. The disturbed equilibrium concentration of the two ionic forms of fluorescein at the water

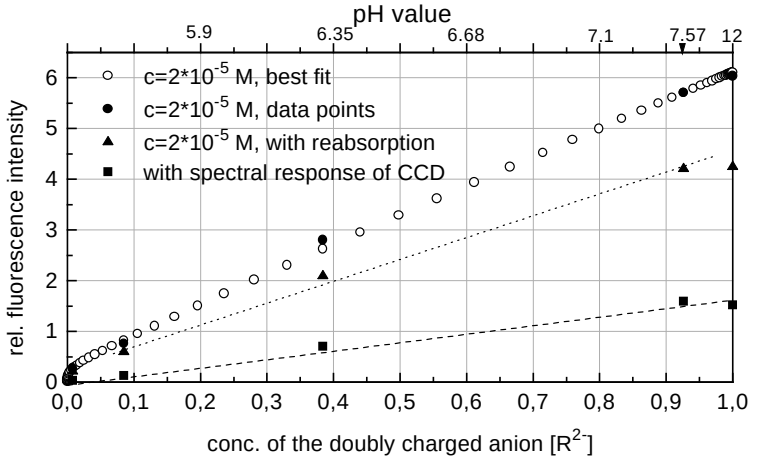

Figure 2: Intensity of the fluorescein fluorescence versus concentration of the doubly charged fluorescein anion. The curves are calculated from literature values for the absorbance at 488 nm [Martin and Lindqvist 1975], fluorescence spectra [Martin and Lindqvist 1975 and Razwadowski 1961] and quantum yields [Razwadowski 1961]. The circles show the response for an ideal system without reabsorption and an ideal CCD response. The upright triangles describe the system with reabsorption in a solution body as it is used in the experiments. The inverted triangles show the response taking into account reabsorption, the spectral response of the CCD and the dichroic mirror.

surface forces a flux of the different ionic forms of HR^- and R^{2-} across the aqueous mass boundary layer into the bulk flow.

This transfer process is equivalent to the transfer of an inert gas without influence by chemical reactions [*Jähne* 1991]. The only chemical reaction takes place directly at the water surface and is on a much shorter time scale than any transportation processes of interest here. Using rate constants by *Yam et al.* [1988] calculations show that 99 % of the possible fluorescein protonation reactions take place within 0.5 μm from the water surface. Although the protonation changes the absorption and fluorescence spectra as well as the quantum yield, the fluorescence intensity is proportional to the concentration of the unprotonated ion over a wide range (see Figure 2). Below pH 8 the nonlinearity is less than 4 %. An alkaline gas (e.g. NH_3) can be used in place of the acidic gas to produce the reverse effect (i.e. the highly fluorescent ions are depleted at the surface).

2.2 The Oxygen Quenching Method

The *oxygen quenching* technique was introduced by *Wolff et al.* [1991]. In this case, the dye concentration is constant, but the concentration of the

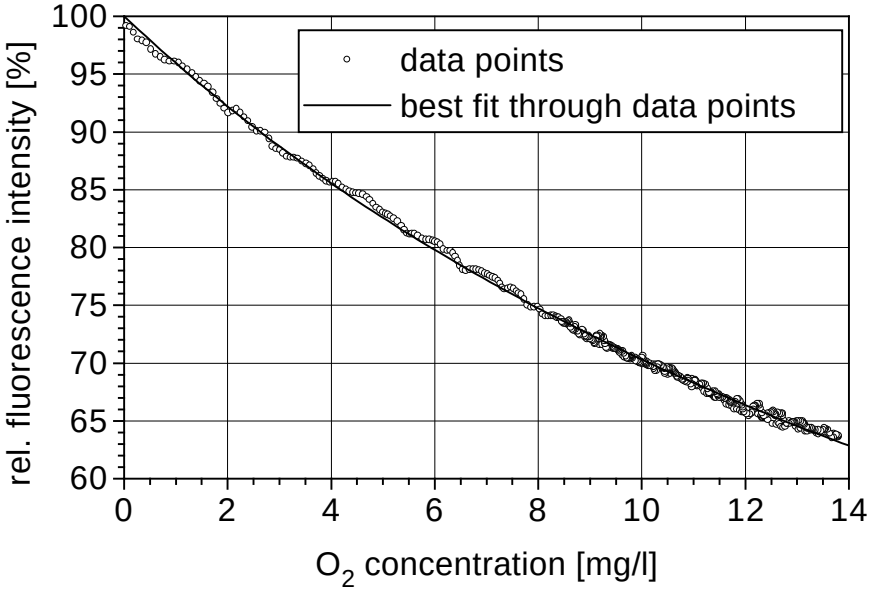

Figure 3: Fluorescence quenching of PBA fluorescence by the presence of dissolved oxygen (data from own experiments, $K = (683 \pm 70)$ l/mol at $T = 298$ K, within the margins of error of the K value first published by Vaughan and Weber [1970]; $K = (645 \pm 79)$ l/mol).

quenching molecule (oxygen) varies in the aqueous mass boundary layer. The presence of oxygen in the water causes the molecules to relax to their ground state through non-radiative collisions. The fluorescence intensity is described by the *Stern-Vollmer equation*:

$$I(c) = \frac{I_0}{1 + Kc}, \tag{1}$$

where I_0 is the fluorescence intensity with no quencher present, K is the quenching constant and c is the concentration of the quencher. The best fluorescent dye for this kind of experiments, described by *Vaughan and Weber* [1970] and *Wolff et al.* [1991], is *pyrene butyric acid* (PBA). It shows an approximately 20% loss of fluorescence intensity with dissolved oxygen concentrations increasing from 0.8 to 8 mg/l (see Figure 3) as is the case for the degased Heidelberg flume.

Experiments show that the two dyes exhibit a high degree of chemical and optical compatibility. Fluorescein fluorescence is neither affected by the presence of PBA in the solution nor significantly stimulated by the N_2 laser. The fluorescein fluorescence also shows only neglectable quenching by oxygen (much less than 1% over the concentration range investigated

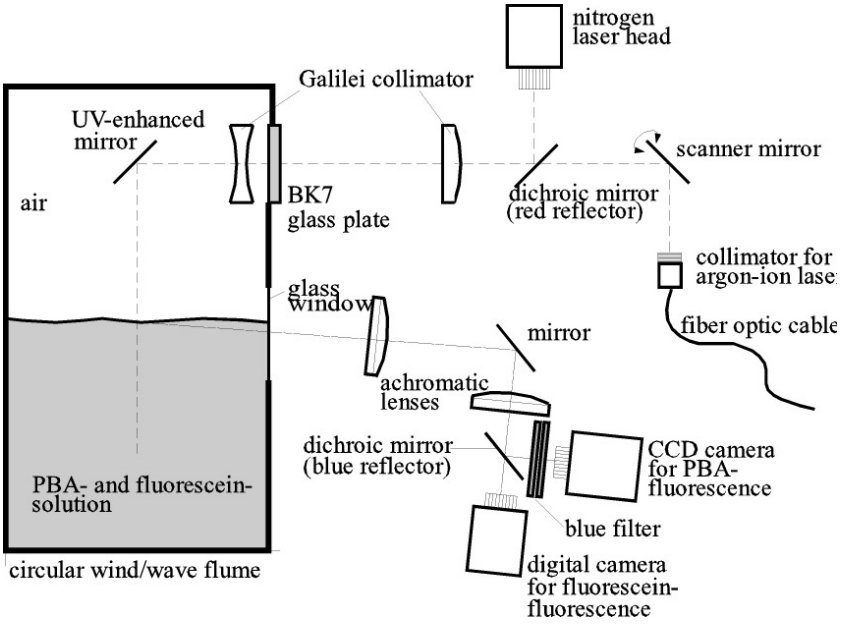

Figure 4: Sketch of the dual tracer experimental setup with imaging CCD-cameras and laser optics. The cameras as well as the laser optics are mounted on an optical wave follower.

here). The PBA fluorescence is not affected by the local pH value of the solution and is not stimulated by the argon ion laser. The possibility of further interferences is discussed in section 4.

3 Experimental Setup

The combined optical arrangement is mounted on an optical wave follower system. The laser optics are mounted on the same base plate as the imaging optics. Figure 4 shows the experimental setup at the circular wind/wave flume of the University of Heidelberg. This facility consists of a 30 cm wide and 70 cm high gas-tight annular channel with an outer diameter of 4 m. Wind is generated by a rotating paddle ring driven by 24 small DC motors. The channel is filled up to a height of 25 cm; so the water and air volumes are 0.88 and 1.6 m^3, respectively. For more details on the flume see *Schmundt et al.* [1995].

A stock solution of PBA and fluorescein in a NaOH solution was prepared (*Wolff et al.* [1991] dissolved the PBA in an organic solvent). This stock solution was then diluted in the flume to give concentrations of 2×10^{-5} M for each of the dyes. In the flume HCl was added to titrate the solution to the fluorescein buffer point at pH 6.5 [*Guyot et al.* 1975]. The surfactant Triton

X-100 was used in a 5×10^{-6} M dilution to suppress waves in these first experiments. At the beginning of the experiment the water was degased. using hollow fiber membranes (Membrane Corp.). The bulk concentration of oxygen in the flume was reduced to less than 1 mg/l. At the water surface the oxygen concentration is equal to the equilibrium concentration (approx. 8.5 mg/l). The PBA fluorescence is stimulated by a focussed nitrogen laser beam at 337 nm with a spot diameter of 200 μm. The oxygen concentration profile across the aqueous mass boundary layer is imaged with a standard NTSC camera. The pulse rate of the laser is 15 Hz resulting in exposure of every fourth field. By averaging over the width of the laser beam, each exposed field results in a one-dimensional profile. The horizontal averaging reduces the noise level. Juxtaposed sequential profiles result in a space-time image. The oxygen profiles were imaged with a 24 μm resolution in the vertical dimension. A stronger laser would be required to allow two dimensional imaging.

Fluorescence for the fluorescein experiment is stimulated by the focused beam of a 1 W argon ion laser (488 nm) piercing the water surface perpendicularly from above. To investigate a two dimensional area the beam is scanned, resulting in a light sheet 6 mm wide and 60 μm deep. Scanning the beam instead of widening it helps to avoid motion blur. Images of the concentration profiles are taken with a digital camera at a rate of 200 frames per second. The spatial resolution of the optical system is 16 μm.

A dichroic mirror allows the beams from the two lasers to travel the same optical path as they strike the water surface. The fluorescence spectra of fluorescein and PBA are separated using a different dichroic mirror in the imaging optical path.

4 Results

The experiments showed that when using HCl as an initiator for the fluorescein technique the two techniques cannot be combined. The PBA fluorescence was found to be severely quenched in the presence of HCl. This is probably due to fluorescence quenching by the chloride ions. Such effects are also known from the literature [*Förster* 1951] for other halogen ions. This results in the fact that two separate approaches have to be followed: a run using only the fluorescein technique with HCl as an initiator and a run using the combined method with NH_3 as an initiator for the fluorescein technique together with the oxygen quenching technique. Both runs were accompanied by a classical mass balance oxygen invasion experiment.

4.1 Fluorescein Experiments

Figure 5 shows a comparison of the boundary layer thicknesses (z_*) measured with fluorescein compared to those calculated from the oxygen invasion transfer velocities. The z_* values from the mass balance experiment

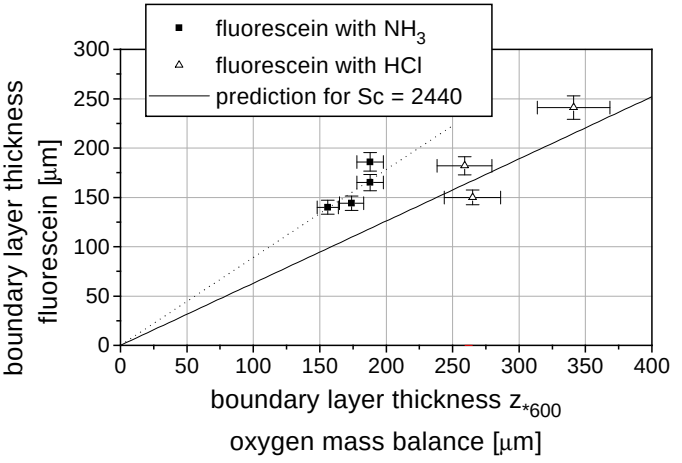

Figure 5: Comparison of the boundary layer thicknesses measured by the fluorescein method with those calculated from the oxygen transfer velocity.

were normalized to Sc = 600. The solid line shows the assumed Sc dependency for a diffusion constant for fluorescein of $D = 3.67 \times 10^{-6}$ cm^2/s [*Hodges and La Mer* 1948]. The z_* values using NH_3 as an initiator deviate significantly from this line. The HCl values agree with this prediction within the margins of error ($\triangle z_* / z_* = 8\%$ for the oxygen mass balance value and $\triangle z_* / z_* = 5\%$ for the fluorescein value). The problem with the NH_3 probably results from the low rate constant for the dissociation reaction $NH_3 + H_2O \leftrightarrow NH_4^+ + OH^-$. The combined profile is affected by both the fluorescein and NH_3 transfer. The small rate constant for NH_3 violates one of the basic assumptions for the feasibility of the fluorescein technique: the time for the protonation reaction must be neglectable compared to any transportation processes. On the other hand this assumption is completely fulfilled for the HCl. More thorough investigations and numerical simulations have to be performed to be able to interpret the profiles obtained with NH_3 as an initiator for the fluorescein flux.

Figure 6 shows a comparison of averaged concentration profiles with the predictions by the small eddy and surface renewal models in dimensionless units. The profiles clearly show better agreement with the profiles for the Schmidt-number exponent 2/3. At this point the concentration profiles cannot clearly distinguish between the predictions for the different models. Nevertheless such a distinction seems to be possible in the future.

Figure 7 shows three consecutive images of the two-dimensional fluorescein field. These have been normalized to the frame of reference of the water surface using image processing techniques. Although almost no waves were present, separated dark streaks indicate that parts of the boundary layer are being swept into the bulk.

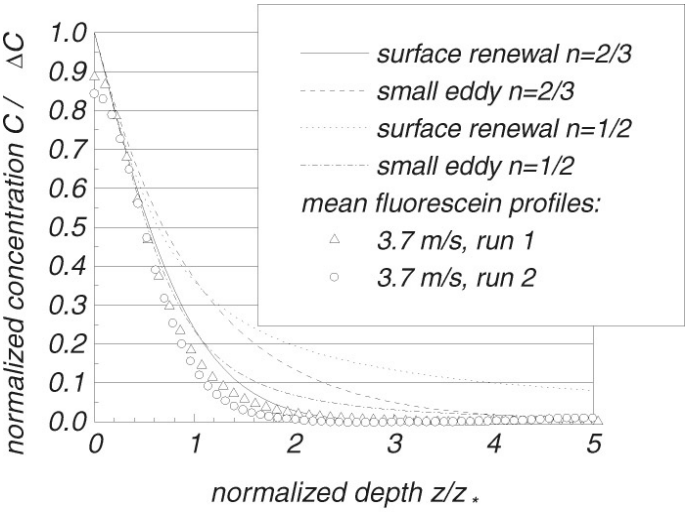

Figure 6: Comparison of the mean concentration profiles for fluorescein (using HCl as an initiator) with the predictions by the small eddy and the surface renewal models. The mean profiles are each averaged over 450,000 single profiles.

4.2 Oxygen Quenching

Figure 8 shows a space time image of the oxygen quenching technique normalized to the frame of reference of the water surface. The signal-to-noise ratio is much worse than for the fluorescein technique. The right hand side of Figure 8 shows a single profile at time 8 s. At this point it seems impossible to evaluate single profiles imaged with a standard CCD camera. Also the time resolution of 15 frames/s impedes the investigation of dynamic processes. A different approach has been taken by *Duke and Hanratty* [1995] imaging single two-dimensional fields with a thermo-electrically cooled *high resolution* camera.

In spite of the noise level mean profiles and mean boundary layer thicknesses can be obtained with the technique used here. Figure 9 shows a comparison of z_* values normalized to Sc = 600 for the oxygen quenching and oxygen mass balance technique. The values agree quite well, although larger differences can be seen for the values measured at 3.6 m/s. All of these values were measured on the same day and the deviation is probably due to a calibration problem with the oxygen probe.

Figure 10 shows a comparison of the averaged oxygen concentration profiles with the small eddy and surface renewal model predictions. As with the fluorescein profiles, the oxygen profiles clearly indicate the expected Schmidt-number exponent 2/3. The profiles also show a flattening at the interface. The flattening at the interface is disturbing because all models predict a sharp concentration change at the interface. Since both techniques

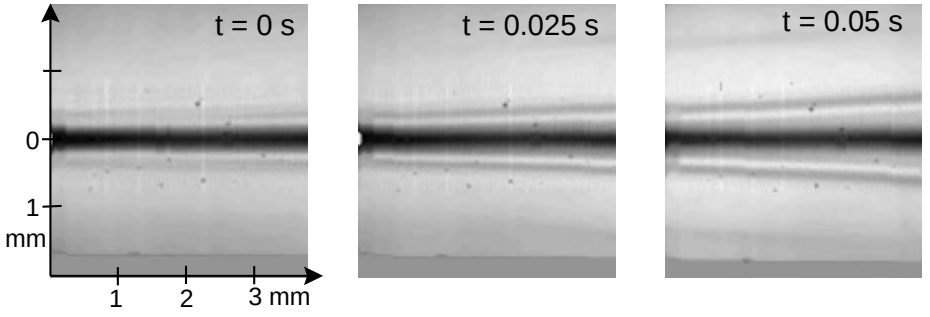

Figure 7: Three out of 1800 images taken with the fluorescein technique using HCl as an initiator. The wind speed is 3.6 m/s coming from the left side at a smooth interface. The aqueous mass boundary layer can be seen as a dark stripe in the middle of the image. The original profile is going down into the bulk. The top part of the image is caused by total reflection at the water surface.

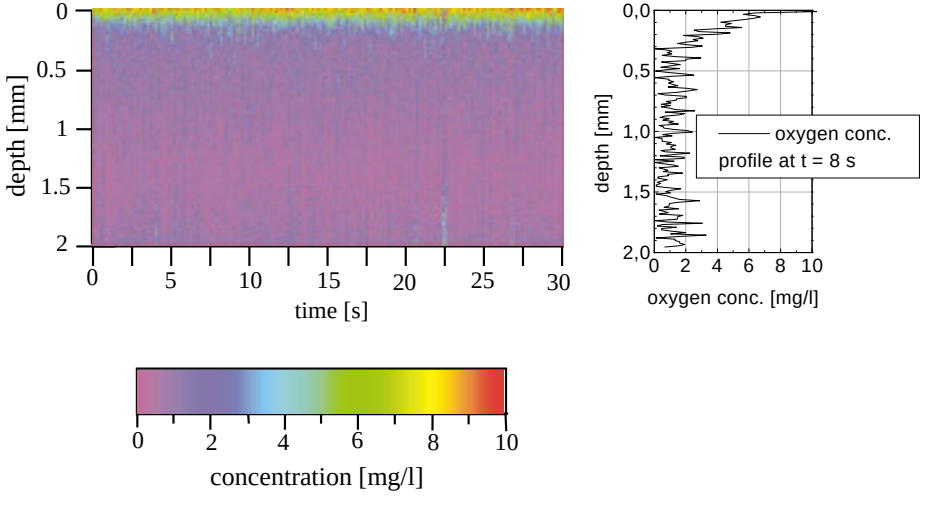

Figure 8: Left: Space time image of the oxygen concentration profile. The aqueous mass boundary layer is visible as a dark layer in the middle of the image. The image is converted to the frame of reference of the water surface using image processing techniques. Right: Cross section through the left hand image at time $t = 8$ s. (For color figure, see Plate 21.)

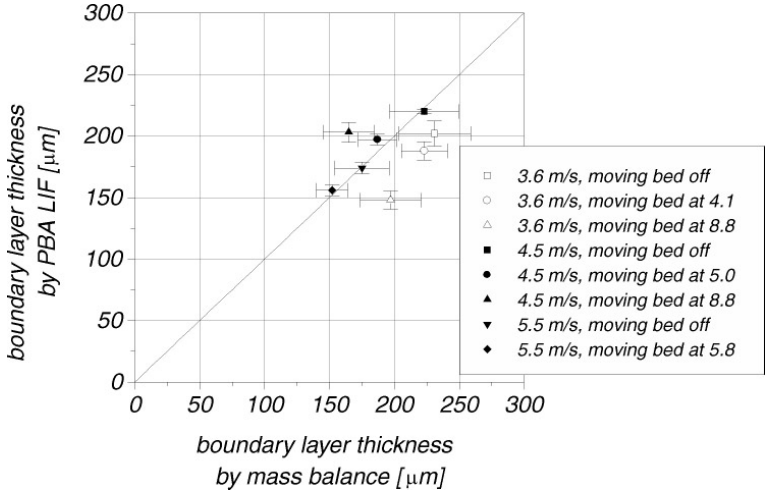

Figure 9: Comparison of the boundary layer thicknesses measured by the oxygen quenching method with those calculated from the oxygen transfer velocity.

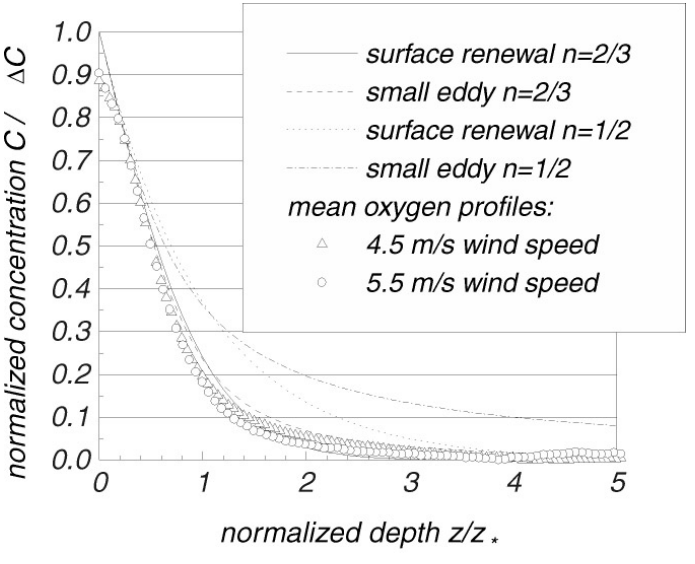

Figure 10: Comparison of the mean oxygen invasion concentration profiles with the predictions by the small eddy and the surface renewal model. The mean profiles are averaged over 16,200 and 10,800 single measurements, i.e. 18 and 12 minutes respectively.

measure such a flattening a chemical reaction of the fluorescein can be ruled out. The flattening is caused either by an optical effect (blur) or a "real" physical effect. The flattening is of the same scale in dimensionless plots although the actual mean boundary layer thicknesses differ by almost a factor of two. This is untypical for optical blur. Furthermore from the measured oxygen concentration in the bulk the surface concentration can be calculated using the Stern-Vollmer equation and the averaged fluorescence profiles. These calculations agree with the values calculated from the Ostwald solubility to within 3%. An optical blur should decrease this calculated surface concentration in the order of 15 to 20%.

5 Conclusions

The fluorescein technique using NH_3 as an initiator shows systematic deviations and needs further investigations. The oxygen quenching technique as well as the fluorescein technique using HCl as an initiator could be verified. For both techniques mean concentration profiles were calculated and compared to model predictions. The dynamic properties of the fluorescein profiles show that parts of the boundary layer are being swept into the bulk. The noise level for the oxygen profiles is too high to allow single profile evaluations. A combination of both techniques at the same time and location is not yet feasible because HCl interferes with the oxygen quenching. For a combination another acid or alkaline gas has to be found.

Acknowledgements

Financial support of this research by the National Science Foundation (Grant OCE9217002) is gratefully acknowledged.

References

Duke, S. R. and T. J. Hanratty, Measurements of the concentration field resulting from oxygen absorption at a wavy air-water interface, *This volume*

Förster, T., Fluoreszenz organischer Verbindungen, Vandenhoeck & Ruprecht, p. 184, 1951.

Hodges, K. C. and V. K. La Mer, Solvent Effects of the Quenching of the Fluorescence of Uranin and Aniline, *Am. Soc.*, **70**, 724, 1948.

Jähne, B., From mean fluxes to a detailed experimental investigation of the gas transfer process, *Air-Water Mass Transfer*, selected papers from the 2nd International Symposium on Gas Transfer at Water Surfaces, September 11–14, 1990, Minneapolis, Minnesota, S. C. Wilhelms and J. S. Gulliver, eds, pp. 244-256, ASCE, New York, 1991.

Guyot G., R. Arnaud et J. Lemaire, Emission des différentes formes de la fluorescéine en solution aqueouse, *J. Chim. Phys.*, **72**, no. 5, 647–653, 1975.

Martin M. M. and L. Lindqvist, The pH dependence of fluorescein fluorescence, *J. Luminescence*, **10**, 381–390, 1975.

Razwadowski M., Effect of pH on the fluorescence of fluorescein solutions, *Acta Phys. Polonica*, **XX** (961), 1853–1854, 1961.

Schmundt D., T. Münsterer, H. Lauer and B. Jähne, The circular wind/wave facility at the University of Heidelberg, *This volume*.

Vaughan W. M. and G. Weber, Oxygen Quenching of Pyrenebutyric Acid Fluorescence in Water, *Biochemistry*, **9**, 464, 1970.

Wolff, L. M., Z.-C. Liu and T. J. Hanratty, A fluorescence technique to measure concentration gradients near an interface, *Air-Water Mass Transfer*, selected papers from the 2nd International Symposium on Gas Transfer at Water Surfaces, September 11–14, 1990, Minneapolis, Minnesota, S. C. Wilhelms and J. S. Gulliver, eds, pp. 210–218, ASCE, New York, 1991.

Yam R., E. Nachliel and E. Gutman, Time resolved proton-protein interaction. Methodology and kinetic analysis, *J. Am. Chem. Soc.*, **110**, 2636–2640, 1988.